WPMAT-CPR(17) 17070

J Riesch et al.

Deformation behaviour of drawn tungsten wire used in tungsten fibre-reinforced tungsten composites

Preprint of Paper to be submitted for publication in Proceeding of 16th International Conference on Plasma-Facing Materials and Components for Fusion Applications

This work has been carried out within the framework of the EUROfusion Consortium and has received funding from the Euratom research and training programme 2014-2018 under grant agreement No 633053. The views and opinions expressed herein do not necessarily reflect those of the European Commission.

Tensile behaviour of drawn tungsten wire used in tungsten fibre-reinforced tungsten composites

J. Riesch[1], A. Feichtmayer[1,2], M. Fuhr[1,3], J. Almanstötter[4], J.W. Coenen[5], H. Gietl[1,2], T. Höschen[1], A. Manhard[1], Ch. Linsmeier[5], R. Neu[1,2]

[1] Max-Planck-Institut für Plasmaphysik, 85748 Garching, Germany
[2] Technische Universität München, 85748 Garching, Germany
[3] Department of Material Science, Glass and Ceramics, University of Erlangen-Nürnberg, Martensstr. 5, Erlangen, Germany
[4] OSRAM GmbH, Corporate Technology CT TSS MTS MET, 86830 Schwabmünchen, Germany
[5] Forschungszentrum Jülich GmbH, Institut für Energie- und Klimaforschung – Plasmaphysik, 52425 Jülich, Germany

E-mail: `johann.riesch@ipp.mpg.de`

Abstract. In tungsten fibre-reinforced tungsten composites (W_f/W) the brittleness problem of tungsten is solved by utilizing extrinsic toughening mechanisms. The properties of the composite are very much related to the properties of the drawn tungsten wire used as fibre reinforcements. Here the high strength and the ductile deformation of tungsten wires are ideal properties faciliating toughening of W_f/W. Tensile tests are used for determining mechanical properties and study the deformation and the fracture behaviour. Tests of drawn wires with a diameter between 150 µm and 16 µm as well as wire electrochemically thinned to a diameter of 5 µm have been performed. Engineering stress-strain curves and microscopical observation are presented whereas the focus is laid on the strength. All fibres show a comparable stress-strain behaviour with necking followed by a ductile fracture. Drawing leads to an increase of strength to 4500 MPa for wire with a diameter of 16 µm. First results on 5 µm thick wire reveal a slight decrease of strength but due to their small size opens new possibilities for the combination of mechanical tests and plasma wall interaction studies .

1. Introduction

Tungsten is the main candidate for highly loaded areas in a future fusion reactor due to its excellent erosion resistance and low H retention as well as high temperature strength and creep resistance combined with a high thermal conductivity and melting point [1]. However, tungsten features an intrinsic brittleness up to a temperature of typically 500 K - 600 K [2] and is prone to operational embrittlement e.g. by grain coarsening [3] or/and neutron irradiation [4]. In tungsten fibre-reinforced tungsten composites (W_f/W) the brittleness problem is solved by utilizing extrinsic toughening mechanisms similar to ceramic fibre-reinforced ceramic composites [5, 6, 7]. The properties of the composite are very much related to the properties of the tungsten wire used as fibre reinforcements [8, 9]. Here the high strength and the ductile deformation of tungsten wires are ideal properties facilitating the toughening in W_f/W. The high strength is important for the bridging effect and ductile deformation allows the dissipation of a substantial amount of energy [10].

The main use of tungsten wire has been for many years the use as filaments in lightning applications [11]. Here a key parameter is the creep resistance at high temperatures which has been significantly improvement by the development of potassium doped material. The main focus of research has been in manufacturing and high temperature stability up to now. However, if used as reinforcements in composites as in W_f/W the performance at lower temperature in general as well as the classical mechanical properties like strength or fracture behaviour are becoming more important.

In this context both pure and potassium doped tungsten wire with a diameter of 150 µm have been investigated in tensile tests at room temperature in the as-fabricated and annealed state [12, 10]. Both wires show comparable behaviour with a high strength and ductility until the elongated fine grain structure gets lost by recrystallisation accompanied by massive grain growth. Recently tensile tests at temperatures up to 600 °C on identical wire revealed a good high temperature strength [13]. In all cases no significant difference in the behaviour of doped and undoped wire is observed. Recently the ductile behaviour has been matter of detailed investigation [14]

The good properties of W wire are attributed to the high deformation state. The thinner the wire the larger the deformation. In general the room temperature ductility of tungsten increases with increasing deformation as firstly described by W.D. Coolidge [15, 16]. The deformation state is a consequence of the typical manufacturing process. The first step in the production of tungsten wire is the preparation of the W powder and the possible doping with potassium. Powder pressing is used to form a green body which is then sintered by direct current to form an ingot. This ingot is then bar rolled and swagged and finally drawn down to the desired diameter of 2 to 4 mm. The wire is subsequently drawn through dies with decreasing size until the final diameter is reached. The drawing temperature starts at 1000 °C and is decreased with decreasing diameter. The reduction in area per drawing step lies between 40 % (at the beginning) and 10 % (in the end). As the strength significantly increases during each drawing steps intermediate annealing steps at a temperature of 1600° are necessary to prevent overworking. Details of the process can be found in [16].

In this contribution we present the results of tensile test at room temperature of commercially available W wire with diameters between 16 µm and 150 µm and wire thinned to 5 µm. Engineering stress-strain curves and microscopical observation are presented. The aim is to compare the mechanical behaviour of the different wire types and provide strength values to support the understanding and future design of W_f/W composites.

2. Experimental

As-fabricated and straightened drawn tungsten wires with diameters between 16 and 150 µm were provided by the OSRAM GmbH, Schwabmünchen (see table 1). The wires were doped with 60-75 ppm potassium . The straightening was down by rolling at elevated temperature . As a diameter reduction by drawing is not possible below 16 µm electrochemical thinning was used to reduce the diameter to the approximately 5 µm. A *16* type fibre is coated by an isolating protective lacquer apart from a 2 mm long region in the centre. For the electro thinning the fibre is mounted electrically conductive onto a rotable sample holder and put into an electrolyte (mixture of NaOH, H_2O and glycerine). The fibre serves as anode surrounded by an annular cathode. Under rotation a current of 7 V leads to a uniform removal of material until the target diameter is reached. It has to be noted that carbon containing remains on the wire led to a partly inhomogeneous abrasion. This contaminants are probably caused by the fabrication process.

The wires were delivered on spools and were cut by a tungsten carbide nipper to a length of 70 - 80 mm . These wire pieces are called fibres in the following. The fibre ends were embedded into a two component epoxy glue (UHU Plus endfest 300). The cross-section in the embedded area is enlarged and thus the probability of fracture in this area is reduced (compare procedure described in [10]). The free space in-between the embedded area defines the measuring length. The measuring length was approximately 25 to 30 mm for all tests. For the thin diameters (*5* and *16*) the fibres were attached to a paper frame allowing an easy handling. The sides of the frame parallel to the fibre were cut after mounting the sample into the testing device.

The tensile tests were performed with a universal testing machine (TIRA Test 2820) at room temperature. A 200 N range load measuring cell was used for the fibres of the type *150* and *150-st* and a 20 N range load cell for thinner wires. For the *150* type fibre the displacement was measured by the machine way. For the other fibres a contactless optical measurement system was established. In this system the fibre is monitored throughout the test by a high speed ccd camera (aquisition rate 10 Hz) combined with a telecentric lens. This lens displays an ortographic view and thus allows the geometrically correct tracking of characteristic points on the object. By detecting the movement of these points the displacement and thus the strain is calculated using a LabView based program. The edges of the epoxy embedding and for the *16* type fibre the edges of the paper frame were used as reference points. For *5-th* fibres the transition points to the thinned centre parts are used. The tensile test were performed in a displacement controlled mode with a constant testing speed of $0.5\,\mu m\,s^{-1}$ for the *5-th* type, of $1\,\mu m\,s^{-1}$ for the *16* type, and of $5\,\mu m\,s^{-1}$ for the other types. The fracture surface of selected samples was investigated using a FEI Helios NanoLab 600 scanning electron microscope (SEM). As a measure for deformation the reduced diameter was determined for selected fibre types using the SEM images .

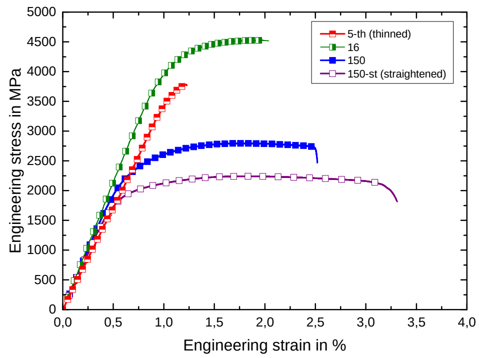

Figure 1. Typical engineering stress - engineering strain curves for *5-th*,*16*,*150* and *150-st* fibres.

3. Results

In all cases comparable stress-strain curves were observed. It has to be noted that due to the very low maximum strength values of about 80 mN for the *5-th* type fibres the determination of the curve in this case was challenging. Typical curves are shown for some fibre types in figure 1. After a region of elastic loading, strain hardening is observed. For the straightened fibre the strain hardening was in general less pronounced. After that a plateau within the maximum load is reached was observed. In this region the stress only changes moderately. For fibres with a diameter larger than 16 µm a faster load drop occurs prior to final fracture. The plateau as well as this larger load drop was not detectable for the *5-th* type fibre. The ultimate strength as well as the reduction in cross-section have been chosen for a quantitative comparison of the different fibre types as they are independent of the strain measurement as measuring the strain is in general a demanding task for thin fibres (see e.g. [10]). An overview of the obtained results is given in table 1. For the as-fabricated wire types a significant increase of strength and cross-section reduction with decreasing diameter is observed except for the fibre *100*. In general the loads are lower for straightened and the thinned wire. Also here the *100-st* shows a different behaviour with a very similar strength to the as-fabricated type.

In figure 2 typical fracture surfaces are shown for *150-th*,*150*,*16* and *5-th* fibres. Necking was observed for all fibres as well as the typical fibrous structure as a result of the knife edge failure of individual grains. The fracture surface of the *150-th*,*150* and *16* type fibres look very similar showing in addition some larger cracks. The *150-th* fibre shows some cleavage fracture near a large crack (see white arrows in figure 2). The thinning did not change this significantly and the fracture surface of the *5-th* fibres look similar but exhibiting a more wrinkled outer face .

Table 1. Overview of tested wire types and results for ultimate strength and reduction of diameter. The uncertainties are calculated as standard deviation of the mean for *5-th* and *16* type fibres and as described in 5 for the other fibre types.

ID	*Diameter in* µm	*Number of valid tests*	*Ultimate strength in* MPa	*Reduction in area in* %	*Preparation state*
5-th	5	3	4055 ± 144	55 ± 2	thinned
16	16	10	4519 ± 10	49 ± 1	as-fabricated
50	50	8	2935 ± 27	-	as-fabricated
50-st	50	8	2405 ± 22	-	straightened
100	101	7	2152 ± 17	-	as-fabricated
100-st	101	7	2167 ± 17	-	straightened
150	150	9	2774 ± 29	37 ± 3	as-fabricated
150-st	149	7	2244 ± 25	(47)*	straightened

**) only one valid measurement*

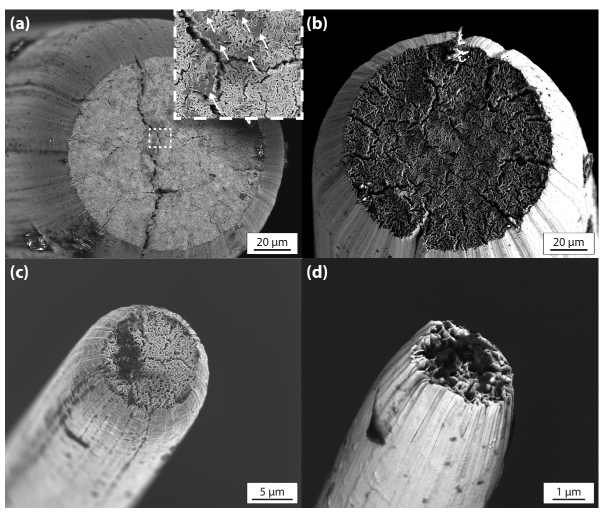

Figure 2. SEM image of a typical fracture surface of (a) *150-st*, (b) *150*, (c) *16* and (d) *5-th* type fibres. All fibres exhibit necking and a fibrous structure caused by the knife edge failure of individual grains. The detail in (a) shows cleavage fracture near a large crack, indicated by white arrows.

4. Discussion

As the diameter decreases the strength increases for the as-fabricated fibres. This can be attributed to the reduction in grain diameter accompanied by grain elongation. The metallurgical background will be discussed later and is also reported here [16] . The reduced strength for the straightened wire can be attributed to the reduced amount of dislocations caused by recovery processes by annealing during the straightening process. This results in a reduced strain hardening effect. A similar reduction in strength for

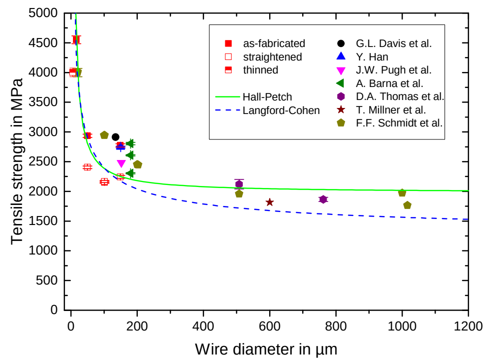

Figure 3. Comparison of strength of drawn tungsten wire with diameter between 16 and 762 µm [10].

fibres with a diameter of 150 µm observed for annealing experiments was attributed to the reduction of dislocations [10, 12]. There is no increase in strength by the diameter reduction from the *16* type fibres to the *5-th* type fibres which is not surprising as the microstructure is not changed during this process. The slightly reduced strength could be a consequence of variations within the fibres. Also the different surface conditions of as-fabricated and electro polished material may have an influence. However, the restricted number of tests has to be taken into account and further tests are planned for a better understanding. The similar strength values for the as-fabricated and straightened fibres with a diameter of 100 µm might be caused by a different fabrication history. As mentioned above intermediate annealing steps are needed during the drawing process. It can easily happen that these steps have been performed at different steps for these two wires. An annealing procedure for the as-fabricated wire later in the drawing process would reduce the strength similar to the annealing during the straightening [16]. Microstructural investigations are planned to compare the amount of disslocations in the two different wire types. In figure 3 the results for ultimate strength are summarized and compared to literature values. It was shown that straightening due to the annealing as well as intermediate annealing steps can have a significant influence on the observed mechanical behaviour and more precisely to the strength. This has to be taken into account if comparing different tension test results. The difference between the here measured as-fabricated and straightened wire of $\Delta\sigma_{\mathrm{u}} = 331 \pm 28\,\mathrm{MPa}$ can be taken as a first estimation of this variation. However, wherever possible the exact fabrication history should be taken into account.

The fracture behaviour with a pronounced necking and the typical fibrous fracture of individual grains is typical for tungsten fibres [17, 10, 12]. The observed larger cracks for the larger fibres were probably caused by surface groves originating of the fabrication process [12, 13]. The reduction in cross-section is similar to literature values for the *150* type fibre [14] and rises for very thin fibres . With respect to the restricted sample number a clear trend for the *5-th* fibres can not be given. The necking in the *150-th* although only measured for one sample corresponds well with the results observed for annealed wire [12]. A reduced dislocation density seems to be beneficial for necking . Whether this can also be the explanation for the thin fibres can be proven by a microstructural analysis. The cleavage fracture occurred in *150-th* fibres has been also observed for annealed wire in [12] and was attributed to a lower present stress. This could also be the case here due to a stress reduction by the large crack nearby . The wrinkling of the *5-th* fibres might be a consequence of the electro polishing reducing surface growths and therefore promote wrinkling rather than the formation of cracks.

As mentioned above the metallurgical reasons for the observed results will be discussed in the following. The characteristic microstructure of drawn tungsten wire shows a high grain boundary area [14, 18, 19, 20] . This suggests the assumption that grain boundaries act as obstacles for dislocation motion and therefore increase the strength (and ductility) of tungsten wire in terms of a grain boundary hardening mechanism. In order to evaluate this assumption, the mechanical properties obtained in the uniaxial tensile tests were analysed. The tensile strength, which is clearly defined as the maximum stress observed in a tensile test, was used for evaluating the strengthening mechanisms of drawn tungsten wire. It is common to plot a mechanical parameter such as the tensile strength against the (mean) grain size of a material in order to study its strengthening behaviour. As an easy to measure parameter with a direct relationship to the grain size the wire diameter was chosen in this study [21, 11] . This can of course only give a first idea as the role of dislocations as well as the role of the fabrication history is neglected. Two different models are used to describe the grain boundary hardening mechanisms. On the one hand, the model by Hall [22] and Petch [23] (Hall-Petch), describing the relation between a mechanical parameter and grain diameter D using the constants σ_0 and k. The related formula with the tensile strength as mechanical parameter and adopted for the wire diameter instead of the grain size is the following:

$$\sigma_{\mathrm{u,HP}}(d) = \sigma_{0,\mathrm{HP}} + \frac{k_{\mathrm{HP}}}{\sqrt{d}} \tag{1}$$

On the other hand, a deviation from equation (1) proposed by Langford and Cohen [24, 25] (Langford-Cohen) was fitted to the experimental data. The difference between the models manifests in a different exponent of the grain size or the wire diameter in this case:

$$\sigma_{\mathrm{u,LC}}(d) = \sigma_{0,\mathrm{LC}} + \frac{k_{\mathrm{LC}}}{d} \tag{2}$$

Only results of wire in the as-produced condition are used for the model description to avoid the influence of the treatment (straightening, thinning) and unknown fabrication history (literature values). The curves of the two models based on these results are plot in figure 3. The two models seem to describe the whole of the strength values similarly well. This is especially true if one takes $\Delta\sigma_{\mathrm{u}}$ as an estimation for an error bar of the unknown fabrication history. Though the Hall-Petch model and the deviations developed later-on were empirical, microstructural meanings of the parameters were found [26, 27]. As it is not depending on the microstructural or geometrical parameter,

Table 2. Parameters for Hall&Petch and Langford&Cohen equations.

	Exponent n	σ_0 *in* MPa	k *in* MPa m^n
Hall-Petch	0.5	1179	12.16
Langford-Cohen	1	1977	0.04

Table 3. Parameters for Hall-Petch and Langford-Cohen equations.

	Geometry	*Yield strength* R_m *in* MPa
[29]	rod	750
[30]	rod	860 ± 50
[31]	nanopillar	≈ 1000

respectively, that is used for analysing grain boundary strengthening, σ_0 can be utilized to check the outcome of the fitting procedure. σ_0 can be interpreted as the friction stress which is needed to move a dislocation in the lattice of the chosen material [26]. Thus among others, the stress required for overcoming the Peierls barrier contributes to this parameter. For the limiting case of the grain size approaching infinity, the parameter σ_0 should be equal to the mechanical property (in this case the tensile strength) of a single crystal [3, 28]. Tensile strengths for tungsten single crystals are shown in table 3. Comparing the literature values for tensile strength of tungsten single crystals and the obtained fitting parameter σ_0, the parameter taken from the Hall-Petch model is close to the literature values whereas that for the Langford-Cohen model is more than twice the value found in literature. Extensive studies revealed that the Hall-Petch model applies, if the majority of grain boundaries are high-angle grain-boundaries [27], while the Langford-Cohen model is more accurate for microstructures mainly comprising low-angle grain boundaries [32]. Thus, it is necessary to study the types of grain boundaries in as-produced drawn tungsten wire for example by performing EBSD (electron backscatter diffraction) measurements. Nevertheless, by comparing the positions of the data points in figure 3 and the curve characteristics, one can clearly state that the high strength of drawn tungsten wire is at least partially due to grain boundary hardening mechanisms.

By using wire with a diameter of 16 µm in W_f/W the bridging effectiveness could be significantly increased due to the significantly increased strength. However, the handling of this very thin wire during the manufacturing process will be challenging. At the moment investigations are ongoing to use this wire as multifilaments in tungsten yarns. This would allow the easy use of the thin wire in the standard production processes. The tensile behaviour of W wire occurs to be very similar for the different tested wire diameters. Also the thinning does not significantly change this. This now opens the possibility to use thin fibres as a measure for dedicated experiments requiring a small size as e.g. irradiation by high energetic ions . In the case of establishing the use of multifilament yarns the study of the filaments would be sufficient to estimate the real material behaviour.

5. Summary and outlook

Tensile tests on tungsten wires with different diameter reveal a strong relationship between strength and diameter as well as fabrication history. The most important findings are:

- Reducing the diameter by drawing generally increases the strength up to 4500 MPa for wire with a diameter of 16 µm.
- Heat treatment as for example performed during straightening leads to a reduction of strength
- The tensile behaviour of W wire is not significantly changed by the reduction of the diameter by drawing.

To investigate the relationship between diameter, grain size and dislocation detailed microstructural investigations are ongoing. Tests of wires with larger diameter will allow expanding the database and thus a better correlation with microstructural models .

Acknowledgements

The authors want to thank G. Matern, M. Balden and S. Elgeti for their assistance in microscopy. This work has been carried out within the framework of the EUROfusion Consortium and has received funding from the Euratom research and training programme 2014-2018 under grant agreement No 633053. The views and opinions expressed herein do not necessarily reflect those of the European Commission.

Appendix

In order to evaluate the accuracy of the measured values describing the mechanical properties of the tungsten wires, an error analysis was performed. Therefore, the equations for the relative error limits resulting from the Gaussian error propagation were utilized. This yields the following formula for the tensile strength R_m of a drawn tungsten wire with an initial diameter d:

$$\Delta\sigma_{\mathrm{u}} = \sigma_{\mathrm{u}} \cdot (\frac{\Delta F}{F} + \frac{2\Delta d}{d}) \tag{3}$$

The tensile strength σ_{u} observed in a tensile test was calculated as the maximum force measured throughout the test related to the wire cross-section. The relative error of the force F, $\frac{\Delta F}{F}$, is specified to be $0,025$ by the manufacturer of the utilized load cell. The second term in equation (3) arises from the contribution of the cross-sectional area of the tested wires, which was approximated to be circular with a diameter d. The error of the wire diameter was calculated from direct measurements for the wire types *150* and *100* (see 1). The error for the remaining wire types were approximated by a parabolic relation between the diameter provided by the wire manufacturer and its scatter.

References

[1] Coenen J W, Antusch S, Aumann M, Biel W, Du J, Engels J, Heuer S, Houben A, Hoeschen T, Jasper B, Koch F, Linke J, Litnovsky A, Mao Y, Neu R, Pintsuk G, Riesch J, Rasinski M, Reiser J, Rieth M, Terra A, Unterberg B, Weber T, Wegener T, You J H and Linsmeier C 2016 *Physica Scripta* **T167** 014002– ISSN 1402-4896 URL `http://stacks.iop.org/1402-4896/2016/i=T167/a=014002`

[2] Lassner E and Schubert W D 1999 *Tungsten - Properties, Chemistry, Technology of the Element, Alloys, and Chemical Compounds* (Kluwer Academic / Plenum Publishers)

[3] Yih S and Wang C 1979 *Tungsten: Source, Metallurgy, Properties, and Applications* (Springer Science+Business Media New York)

[4] Barabash V, Federici G, Rödig M, Snead L and Wu C 2000 *Journal of Nuclear Materials* **283–287** 138–146 ISSN 0022-3115 URL `http://www.sciencedirect.com/science/article/pii/S0022311500002038`

[5] Riesch J, Höschen T, Linsmeier Ch, Wurster S and You J H 2014 *Physica Scripta* **T159** 014031– ISSN 1402-4896 URL `http://stacks.iop.org/1402-4896/2014/i=T159/a=014031`

[6] Riesch J, Coenen J, Gietl H, Höschen T, Mao Y, Linsmeier Ch and Neu R 2016 Tungsten fibre-reinforced tungsten composite - development of a new high performance material *Proceedings of the 17th European Conference on Composite Materials* iSBN 978-3-00-053387-7

[7] Linsmeier r C, Rieth M, Aktaa J, Chikada T, Hoffmann A, Hoffmann J, AHouben, Kurishita H, XJin, Li M, Litnovsky A, SMatsuo, M?̈uller A, Nikolic V, Palacios T, Pippan R, DQu, Reiser J, Riesch J, Shikama T, Stieglitz R, Weber T, Wurster S, You J H and Zhou Z 2016 *Nuclear Fusion* Accepted

[8] Riesch J, Buffiere J Y, Höschen T, di Michiel M, Scheel M, Linsmeier Ch and You J H 2013 *Acta Materialia* **61** 7060–7071 ISSN 1359-6454 URL `http://www.sciencedirect.com/science/article/pii/S1359645413005557`

[9] Gietl H, Riesch J, Coenen J, Höschen T, Linsmeier r C and Neu R 2017 *Fusion Engineering and Design* – ISSN 0920-3796

[10] Riesch J, Han Y, Almanstötter J, Coenen J W, Höschen T, Jasper B, Zhao P, Linsmeier Ch and Neu R 2016 *Physica Scripta* **T167** 014006–

[11] Schade P 2010 *International Journal of Refractory Metals and Hard Materials* **28** 648–660 ISSN 0263-4368 URL `http://www.sciencedirect.com/science/article/pii/S0263436810000752`

[12] Zhao P, Riesch J, Höschen T, Almannstötter J, Balden M, Coenen J, Himml R, Pantleon W, von Toussaint U and Neu R 2017 *International Journal of Refractory Metals and Hard Materials* Submitted

[13] Terentyev D, Riesch J, Lebediev S, Bakaeva A and Coenen J 2017 *International Journal of Refractory Metals and Hard Materials* **66** 127–134 ISSN 0263-4368

[14] Riesch J, Almanstötter J, Coenen J W, Fuhr M, Gietl H, Han Y, Höschen T, Linsmeier Ch, Travitzky N, Zhao P and Neu R 2016 *IOP Conf. Series: Materials Science and Engineering* **139**

[15] Coolidge W D 1913 Tungsten and method of making the same for use as filaments of incandescent electric lamps and for other purposes

[16] Mullendore J 1989 *The Metallurgy of Doped/Non-Sag Tungsten* (Elsevier) chap The technology of doped-tungsten wire manufacturing, pp 61–82

[17] Leber J, Tavernelli J, White D and Hehemann R 1976 *Journal of Less-Common Metals* **48** 119–133

[18] Meieran E and Thomas D 1965 *Transactions of the Metallurgical Society of AIME* **233** 937–943

[19] ABarna, IGaal, OGeszti-Herkner, GyRadnoczi and LUray 1978 *High Temperatures - High Pressures* **10** 197–205

[20] Walter J L and Koch E F 1991 *Journal of Materials Science* **26** 505–509 ISSN 1573-4803 URL `http://dx.doi.org/10.1007/BF00576550`

[21] Ripoll M R 2009 *Drawing of Tungsten Wires: Microstructure, Mechanical Properties and Longitudinal Cracks* Ph.D. thesis Institut f"ur Werkstoffkunde I:Institut f"ur Zuverl"assigkeit von Bauteilen und Systemen Universit"at Karlsruhe

[22] Hall E O 1951 *Proceedings of the Physical Society. Section B* **64** 747– ISSN 0370-1301 URL `http://stacks.iop.org/0370-1301/64/i=9/a=303`

[23] Petch N 1953 *Journal of Iron and Steel Research International* **174**

[24] Langford G and Cohen M 1969 *ASM Trans Quart* **62** 623–638

[25] Langford G and Cohen M 1970 *Metallurgical and Materials Transactions* **1** 1478–1480

[26] Hirth J P 1972 *Metallurgical Transactions* **3** 3047–3067 ISSN 1543-1916 URL `http://dx.doi.org/10.1007/BF02661312`

[27] Li Y, Bushby A J and Dunstan D J 2016 *Proceedings of the Royal Society A: Mathematical, Physical and Engineering Science* **472** – URL `http://rspa.royalsocietypublishing.org/content/472/2190/20150890.abstract`

[28] Gottstein G 2007 *Physikalische Grundlagen der Materialkunde* (Springer Verlag Berlin Heidelberg)

[29] URL `https://www.americanelements.com/tungsten-single-crystal-7440-33-7`

[30] Garfinkle M 1965 Room-temperature tensile behaviour of ¡100¿ oriented tungsten single crystals with rhenium in dilute solid solution NASA Technical Note 20060516196 Lewis Research Center

[31] Kim J Y, Jang D and Greer J R 2010 *Acta Materialia* **58** 2355–2363 ISSN 1359-6454 URL `http://www.sciencedirect.com/science/article/pii/S1359645409008647`

[32] Lesuer D R, Syn C K and Sherby O D 2010 *Journal of Materials Science* **45** 4489–4894